Journal of Power Sources 205 (2012) 516–524

Contents lists available at SciVerse ScienceDirect

Journal of Power Sources

journal homepage: www.elsevier.com/locate/jpowsour

Constant-current regulator-based battery-supercapacitor hybrid architecture for high-rate pulsed load applications☆,☆☆

Donghwa Shin[a], Younghyun Kim[a], Yanzhi Wang[b], Naehyuck Chang[a,*], Massoud Pedram[b]

[a] Dept. of EECS/CSE, Seoul National University, Republic of Korea
[b] Dept. of EE, University of Southern California, USA

ARTICLE INFO

Article history:
Received 28 September 2011
Received in revised form 1 December 2011
Accepted 20 December 2011
Available online 30 December 2011

Keywords:
Li-ion battery
Supercapacitor
Rate-capacity effect
Constant-current regulator

ABSTRACT

Modern batteries provide high discharging efficiency, but the rate capacity effect in these batteries drastically decreases the discharging efficiency as the load current increases. Electric double layer capacitors, or simply supercapacitors, have extremely low internal resistance, and a battery-supercapacitor hybrid may mitigate the rate capacity effect for high pulsed discharging current. However, a hybrid architecture comprising a simple parallel connection does not perform well when the supercapacitor capacity is small, which is a typical situation because of the low energy density and high cost of supercapacitors.

This paper presents a new battery-supercapacitor hybrid system that employs a constant-current regulator isolating the battery from supercapacitor to improve the end-to-end efficiency from the battery to the load while accounting for the rate capacity effect for the Li-ion batteries and the conversion efficiency data for the regulator. We optimize the system in terms of a delivered energy density which is an end-to-end energy delivery per unit volume of the energy storage elements. We evaluate the delivered energy density with the aid of detailed simulations and develop a design space exploration algorithm based on the characteristics of the proposed architecture. We achieve 7.7% improvement in deliverable energy density over conventional parallel connection of battery and supercapacitor.

1. Introduction

Rate capacity effect in batteries significantly degrades their discharging efficiency under high load currents. Electronic systems commonly exhibit large fluctuation in the load current, which defy the maximum discharging capacity of batteries. Typical electronic systems determine the battery size based on their expected average power consumption, and thus a large pulsed discharging current with peak greatly exceeding the average value can significantly shorten the battery service life in a charge–discharge cycle. Therefore, in battery-powered electronics, we need to reduce the peak current draw.

Electric double layer capacitors, more commonly known as supercapacitors, are widely exploited to mitigate such load current fluctuations in the batteries. They have a superior cycle efficiency, which is defined as the ratio of the energy output to energy input, which reaches almost 100%, and so they are suitable for energy storage in situation with frequent charge–discharge cycles. In a battery-supercapacitor hybrid system, the supercapacitor can store surplus energy from the battery during low load demand periods, and provide required extra current during high load demand period.

Generally, the larger the supercapacitor is, the higher the energy efficiency will be. However, supercapacitors have two significant disadvantages in terms of their volumetric energy density and dollar cost per unit of stored energy compared to the batteries. For portable applications where the size is a constraint and cost is a factor, size of the supercapacitor should be minimized while achieving a reasonable energy efficiency.

Another concern is the terminal voltage variation coming from the characteristics of a capacitor. The terminal voltage of the supercapacitor is linearly proportional to the supercapacitor's state of charge. The terminal voltage increases or decreases dynamically as the supercapacitor is charged or discharged. The variation of the supercapacitor terminal voltage is much higher than that of ordinary batteries. As a result, the efficiency of power converters,

☆ This work is supported by the Brain Korea 21 Project and Mid-career Researcher Program through NRF Grant funded by the MEST (No. 2010-0017680). The ICT at Seoul National University provides research facilities for this study.

☆☆ This work was partly presented in Design Automation and Test in Europe (DATE) 2011 [1].

* Corresponding author at: 599 Kwanak-gu Kwanak Road, Seoul 151-741, Republic of Korea. Tel.: +82 2880 1834; fax: +82 2884 1834.
E-mail addresses: dhshin@elpl.snu.ac.kr (D. Shin), yhkim@elpl.snu.ac.kr (Y. Kim), yanzhiwa@usc.edu (Y. Wang), naehyuck@elpl.snu.ac.kr (N. Chang), pedram@usc.edu (M. Pedram).

0378-7753/$ – see front matter © 2011 Elsevier B.V. All rights reserved.
doi:10.1016/j.jpowsour.2011.12.043

which are connected to a supercapacitor varies significantly due to the potentially large difference in their input and output voltage levels.

To optimize the battery-supercapacitor hybrid for portable applications, the energy efficiency and energy density must be considered simultaneously. More precisely, we propose a new battery-supercapacitor hybrid energy storage system that employs a constant-current regulator. The regulator isolates the battery from the supercapacitor to maximize the deliverable energy density, i.e., the end-to-end energy delivery per unit of volume of energy storage elements, while the rate capacity effect of Li-ion batteries and the conversion efficiencies of the regulator are addressed. We develop a design space exploration algorithm based on the characteristics of the proposed architecture to derives the magnitude of the charging current and the capacitance of the supercapacitor. The algorithm aims at maximizing the deliverable energy density for a given load profile, power converter efficiency models, supercapacitor and battery specifications.

The rest of the paper is organized as follows. Section 2 introduces previous research on the battery-supercapacitor hybrid systems. Section 3 presents proposed hybrid system and compares to the conventional one. Section 4 details the simulation models and states the optimization problem with solution method. Section 5 introduces the implementation of the proposed architecture, and Sections 6 presents the experimental results using the implemented board.

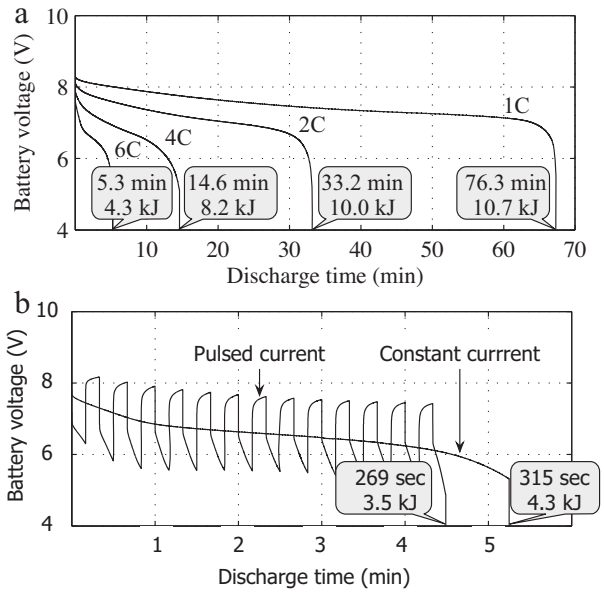

Fig. 1. Discharging a 350 mAh 2-cell Li-ion battery with (a) discharging at a constant current of 1 C, 2 C, 4 C, and 6 C and (b) discharging at a 6 C constant current and 12 C pulsed current of a 20 s period and a 50% duty cycle.

2. Related work

Supercapacitors are widely used for energy storage in various applications. Specifically, supercapacitors are gaining more attention as electrical energy storage elements for renewable energy sources which tend to have a high charge–discharge cycle frequency, and demand high cycle efficiency and good depth-of-discharge (DOD) properties [2].

Relevant previous researches have mainly focused on relieving the load fluctuation to mitigate the rate capacity effect. For example, The authors of [3–5] consider the rate capacity effect in scheduling real-time tasks. It has been shown that taking the rate capacity effect into account also enhances the service life of sensor networks [6]. However, these approaches are justified only when the power management policy can change the load current. Unfortunately, many battery-powered systems including those where the primary source of power consumption is the analog circuits, such as radio amplifiers, provide little freedom to significantly shave the load current to mitigate the rate capacity effect.

There are several related battery-supercapacitor hybrid architectures in the literature on hybrid electric vehicles (HEVs). For example, a bidirectional converter based approach is introduced for the regenerative brake equipped HEVs [7]. A DC power bus based general architecture for the battery-supercapacitor hybrid system is described in [8]. However, it is difficult to directly apply these architectures to portable applications because they are designed for the HEV which involve high-power operation. Different from the HEV, many other factors such as size, weight, cost, and circuit complexity must be addressed in portable battery-powered system.

A supercapacitor in parallel with a Li-ion battery forms a hybrid energy storage that supports a higher rate of discharging current thanks to the high power density of the supercapacitor [9], and thus reduces the impact of the rate capacity effect. Under pulsed load conditions, the supercapacitor acts as a filter that relieves peak stresses on the battery. This type of parallel battery-supercapacitor connection storage has been characterized and evaluated by the use of Ragone plots with pulsed load current and compared with the battery-alone systems in [10]. A simplified model, which helps theoretical analysis in terms of performance enhancement of this hybrid storage, is provided in [11]. Duty ratio, capacitor configuration and pulse frequency play important roles in performance optimization of such a hybrid storage [12].

3. Battery-supercapacitor hybrid system

3.1. Rate capacity effect of Li-ion batteries

We measure the voltage of the Li-ion battery for different discharging currents to show the impact of rate capacity effect on the battery capacity. Fig. 1(a) shows the voltage drop and total amount of delivered energy from the battery with a constant discharging current of 1 C, 2 C, 4 C, and 6 C, when using 2-cell series Li-ion GP1051L35 cells [13]. The discharging efficiency (defined as the ratio of energy delivered from the battery to the load to the nominal energy storage in that battery) at 6 C load current is merely 40% of the 1 C discharging efficiency. In practice, intermittent large amount of discharging current is often applied to batteries due to significant load current fluctuation of a typical battery-powered electronics circuit or systems.

Furthermore, as presented in Fig. 1(b), drawing a pulsed current of 12 C with a 50% duty cycle, which is 6 C on average, results in only 81.3% delivered energy and a shorter service life compared to drawing a constant current of 6 C. This example clearly demonstrates the need of the peak current reduction.

In this paper, we target the high-rate pulsed load applications which tend to seriously reduce the battery service life due to the rate capacity effect. For instance, a US Army radio power amplifier with the output power of 50 W such as AN/VRC-103(V)1 [14] draws up to about 500 W power from a battery unit whenever the PTT (push to talk) of a radio transceiver is applied. The typical scenario for a radio transceiver is repetition of receiving, transmitting and standby, and thus, the battery intermittently experiences a large amount of current draw during the transmission period.

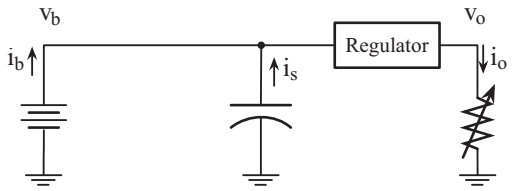

Fig. 2. Parallel connection architecture.

3.2. Parallel connection

A battery-supercapacitor hybrid shown in Fig. 2 is an intuitive way of reducing the effect of load fluctuation on the supplied voltage level. The supercapacitor connected in parallel acts as a low pass filter that prunes out rapid voltage changes. The battery-supercapacitor hybrid is thus effective in mitigating the rate capacity effect for intermittent (rather than continuous) high load current. The supercapacitor shaves the short duration, but high amplitude load current spikes and makes a wider duration but lower amplitude current, which subsequently results in better energy efficiency due to lower rate capacity effect in the Li-ion batteries.

In the parallel connection configuration, the filtering effect of the supercapacitor is largely dependent on its capacitance. A larger capacitance results in better filtering effect. As a result, the parallel connection has a limited ability to reduce the rate capacity effect in the Li-ion battery when the capacitance value of the supercapacitor is not sufficiently large. Unfortunately, due to the volumetric energy density and cost constraints in its practical deployment, the supercapacitor capacitance is generally rather small.

3.3. Constant-current regulator-based architecture

We introduce a new hybrid architecture using a constant-current regulator (cf. Fig. 3) to overcome the disadvantage of the conventional parallel connection hybrid architecture. The constant current regulator separates the battery from the supercapacitor.

The supercapacitor in the parallel connection basically reduces the voltage variation, not the current variation. SPICE simulation results reported in Fig. 4 show that, in the parallel connection, the battery current exhibits a relatively larger variation than the battery voltage. In particular, as the load current (i_o) changes from valley to peak, the battery discharging current (i_b) also changes considerably and nearly reaches the peak load current (cf. Fig. 4(a)). The constant-current regulator-based architecture maintains a desired amount of the charging current regardless of the state of charge of the supercapacitor whereas, in the conventional parallel connection configuration, the charging current is not controllable and varies greatly as a function of the state of charge of the supercapacitor. Current from the supercapacitor (i_s) compensates the difference between the battery and load. Consequently, the proposed hybrid architecture reduces variation in the battery discharging current even with a small supercapacitor.

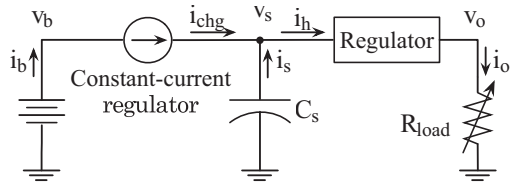

Fig. 3. Constant-current regulator-based architecture.

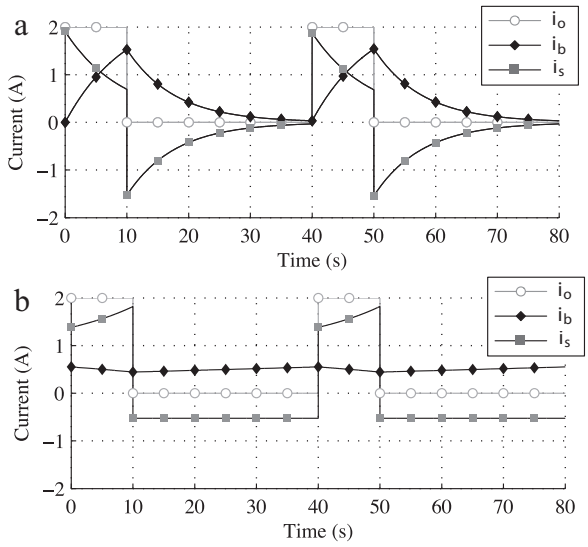

Fig. 4. Current response of the constant-current regulator-based architecture with pulsed load. (a) Current responses of the battery and supercapacitor to the load current pulse in the parallel connection. (b) Current responses of the battery and supercapacitor to the load current pulse in the proposed constant-current regulator-based architecture.

4. Design and optimization of constant-current regulator-based architecture

There are several problems that must be addressed in order to develop a constant-current regulator-based system. With fixed supercapacitor charging current, the amount of delivered power from the battery to the load will depend on the terminal voltage of the supercapacitor. Therefore, to deliver enough power to the supercapacitor, the supercapacitor need to be charged up to certain voltage at initial state. Next, the charging current and the terminal voltage of the supercapacitor should be carefully controlled to achieve efficient and stable operation.

The value of the supercapacitor charging current must be carefully set because it greatly affects the efficiency of the system. The terminal voltage of the supercapacitor determines the amount of power that is transferred from the battery to the supercapacitor at a fixed charging current. The terminal voltage of the supercapacitor must thus be maintained within a proper range in order to meet the load power demand. If supercapacitor's terminal voltage is too high, excessive power will be transferred from the battery to the supercapacitor. In such a case, the terminal voltage continuously rises until some other circuit element pinches off the voltage rise at that terminal. On the other hand, if the supercapacitor's terminal voltage is too low, then the load demand may not be met. To maintain the system in a stable operational condition, the optimal charging current and initial terminal voltage of the supercapacitor must be obtained.

In this section, we will introduce a simulation models with measured parameters, a problem statement, and a solution method to obtain the maximum deliverable energy density.

4.1. Simulation models

4.1.1. Li-ion battery

Battery models for the electronic systems have extensively been studied during the past few decades. We have found many analytical models based on electrochemical process modeling and analysis [15,16], but the electrochemical battery models are too complicated to be used for the system-level design of electronics. Rather, battery

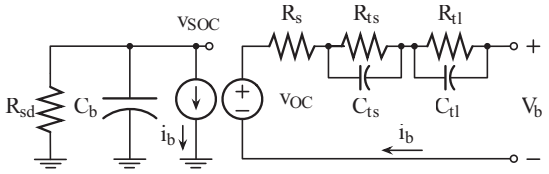

Fig. 5. Li-ion battery equivalent circuit model.

models in the form of an electric circuit are much more suitable for this purpose [17,18].

We import a circuit model of the Li-ion battery from [18] as shown in Fig. 5. This includes a runtime-based model as well as a circuit-based model for accurate capturing of the battery service life and *I–V* characteristic. We can describe the behavior of a Li-ion battery with the equivalent circuit and the following non-linear equations.

$$\begin{aligned} &v_{OC} = b_{11}e^{b_{12}v_{SOC}} + b_{13}{v_{SOC}}^3 + b_{14}{v_{SOC}}^2 + b_{15}v_{SOC} + b_{16},\\ &R_s = b_{21}e^{b_{22}v_{SOC}} + b_{23}, R_{ts} = b_{31}e^{b_{32}v_{SOC}} + b_{33},\\ &C_{ts} = b_{41}e^{b_{42}v_{SOC}} + b_{43}, R_{tl} = b_{51}e^{b_{52}v_{SOC}} + b_{53},\\ &C_{tl} = b_{61}e^{b_{62}v_{SOC}} + b_{63}, C_b = 3600 \cdot Capacity, \end{aligned} \tag{1}$$

where b_{ij} are empirically extracted regression coefficients, while *Capacity* denotes the nominal energy capacity of the battery. Notice that all circuit model component values, such as value of R_s and R_{ts}, are easily calculated from these equations based on v_{SOC} and *Capacity* data.

4.1.2. Supercapacitor

Supercapacitors have superior characteristics over batteries in terms of their cycle efficiency. The cycle efficiency, which is defined as the ratio of the energy input to energy output of an electrical energy storage element, reaches almost 100% [2]. We model the supercapacitor by a connection of various circuit elements. More precisely, the equivalent circuit model incorporates a transmission line behavior, a parasitic inductor model, a charge redistribution element, and a self-discharging current model [19].

We have simplified the complex model of [19] to the circuit model shown in Fig. 6 for fast simulation while preserving accuracy under the actual operating condition of the hybrid system. The load pulse period range of the target application system is from a few seconds to a few tens of seconds and the output converter switching frequency is a few hundreds kHz. Therefore, the charge redistribution and the self-discharge phenomena can safely be ignored. The resonance behavior is also neglected because most supercapacitor terminal behavior occurs under 20 Hz according to a spectral analysis performed through SPICE simulation. As a result, the proposed simplified electric model is composed of a series inductor L_s, an access resistor R_{acc} which physically corresponds to the resistance of the device terminals, a capacitor C_{acc} and a non-linear transmission line with voltage dependent capacitors. Finally, the transmission line is approximated by the simple RC section, R_1 and C_1.

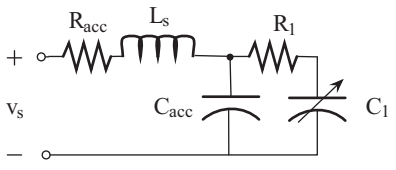

Fig. 6. Simplified supercapacitor equivalent circuit model.

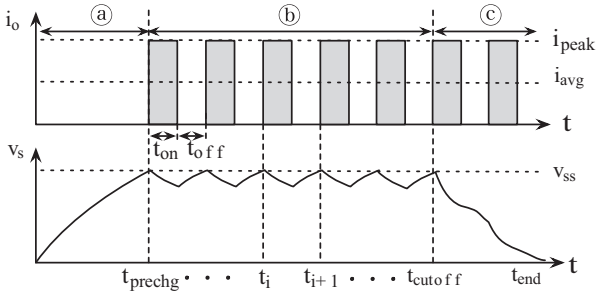

Fig. 7. Pre-charging and steady-state operation of supercapacitor.

4.1.3. Switching DC–DC converter

Switching DC–DC converters are used to transfer power between two different voltage levels. They exhibit a higher efficiency than linear regulators. Batteries and supercapacitors, which have variable terminal voltages that are set according to their state of charge, are commonly paired with switching DC–DC converters to supply a regulated current or a regulated voltage level to the load.

The switching DC–DC converter efficiency is defined as

$$\eta_{converter} = \frac{P_{out}}{P_{in}} = \frac{P_{in} - P_{converter}}{P_{in}}, \tag{2}$$

where $P_{converter}$ denotes the power consumed by the converter, which comprises the conduction losses, gate-drive losses, and controller power dissipation. P_{in} and P_{out} are the input power and output power of the converter, respectively. We import a power model of the switching DC–DC converter from [20]. Based on this model, the power dissipation of a switching DC–DC converter depends strongly on the input voltage v_i, output voltage v_o, and output current i_o as follows:

$$\begin{aligned} P_{converter} &= P_{conduction} + P_{gate} + P_{controller} = {i_{out}}^2(DR_{sw1}\\ &+ (1-D)R_{sw2} + R_L) + \frac{1}{3}\left(\frac{1}{2}\Delta i_L\right)^2(DR_{sw1} + (1-D)R_{sw2} + R_L + R_C)\\ &+ v_{in}f_s(Q_{sw1} + Q_{sw2}) + v_{in}I_{ctrl}, \end{aligned} \tag{3}$$

where P_{gate} is the power consumed in the switches SW_1 and SW_2; $P_{controller}$ is the power consumed by the control logic; v_{out} is the output voltage; i_{out} is the output current; v_{in} is the input voltage; i_L is the current through the inductor L; f_s is the switching frequency of the switches; R_L is the parasitic resistance of the inductor L; R_C is the parasitic resistance of the output capacitor C; R_{sw1} is the turn-on resistance of the switch SW_1; R_{sw2} is the turn-on resistance of the switch SW_2; Q_{sw1} is the gate charge capacity of the switch SW_1; Q_{sw2} is the gate charge capacity of the switch SW_2; I_{ctrl} is the required current of the control logic; D is the switching duty determined by the ratio of input and output voltage.

4.1.4. Load

We assume that the load is modeled by a periodic pulsed train with a regulated voltage value. This is a widely adopted load model used to evaluate the performance of a power source including batteries [9,11,21,22].

Fig. 7 shows the load profile, which is given by

$$i_o = \begin{cases} i_{peak} & \text{if} \quad t_i \le t < t_i + t_{on},\\ i_{idle} & \text{if} \quad t_i + t_{on} \le t < t_{i+1}, \end{cases} \tag{4}$$

where i_{peak} is the peak amplitude of the current pulses; i_{idle} is the load current at idle time; t_i is the start time of the ith pulse; and

Table 1
Extracted parameters for the battery, supercapacitor, and converter models.

Battery					
b_{11}	−0.669	b_{12}	−16.208	b_{13}	−0.035
b_{14}	1.280	b_{15}	−0.399	b_{16}	7.553
b_{21}	0.104	b_{22}	−4.325	b_{23}	0.344
b_{31}	0.151	b_{32}	−19.602	b_{33}	0.188
b_{41}	−72.389	b_{42}	−40.832	b_{43}	102.803
b_{51}	2.071	b_{52}	−190.412	b_{53}	0.203
b_{61}	−695.302	b_{62}	−110.630	b_{63}	611.504
Supercapacitor					
L_s	0.93 μH	R_{acc}	34 mΩ	C_{acc}	0.8 F
R_1	68 mΩ	C_1			$(7.2 + 0.616 \cdot v_s)$ F
Regulator					
R_{sw1}	25 mΩ	R_{sw2}	25 mΩ	R_L	39 mΩ
R_C	100 mΩ	f_s	500 kHz	Q_{sw1}	60 nF
Q_{sw2}	60 nF	I_{ctrl}	4 mA		

finally, t_{on} and t_{off} are the time durations of the high and low current levels, respectively.

4.2. Simulation model parameter extraction

We obtain the discharging characteristics of Li-ion battery by measuring and extracting the regression coefficients for (1). Table 1 shows the parameters for the GP1051L35 Li-ion cell 2-cell series battery pack of 350 mAh capacity, NessCap supercapacitor ESHSR0010C0-002R7 of 10 F capacitance [23], and Linear Technology LTM4607 converter. We validate the battery, supercapacitor, and the converter model with the measurement result of various pulsed discharging and constant discharging currents.

4.3. Optimization problem setup

The supercapacitor needs to be pre-charged up to a certain voltage level before supplying power to the load as illustrated in interval ⓐ of Fig. 7. Of course, we will use part of the pre-charged energy in the supercapacitor after the battery cut-off time, t_{cutoff} (which denotes the time after which the battery's remaining capacity fall below 20%). However, during intervals ⓐ and ⓒ in Fig. 7, the large difference between input and output voltage causes large switching DC–DC converter loss. We consider this amount of energy to calculate the end-to-end energy efficiency. The amount of reusable energy which is available for the load from the pre-charged energy in the supercapacitor is given by

$$E_{reusable} = \int_{t_{cutoff}}^{t_{end}} i_o v_o \, dt. \tag{5}$$

During interval ⓑ in Fig. 7 we have steady-state operation with periodic pulsed load and constant charging current. We need to make the supercapacitor voltage at the start time of the high current time period equal to the voltage at the end time of the low current time period. We can thus represent the steady-state condition as

$$v_{ss} = v_s(t_i) = v_s(t_{i+1}), \tag{6}$$

where t_i denotes the start time for each load pulse period.

Different charging currents cause the proposed hybrid architecture to operate at different steady states under the same pulsed load. Notice that since the charging current and the supercapacitor terminal voltage affect the efficiency of the switching DC–DC converters, we must find not only the optimal capacitance value but also the optimal charging current.

The amount of energy delivered to the load is given by

$$E_{ss} = \int_{t_{prechg}}^{t_{cutoff}} i_o v_o \, dt = \int_{t_{prechg}}^{t_{cutoff}} \eta_{reg} i_h v_s \, dt, \tag{7}$$

where η_{reg} is the power conversion efficiency of the voltage regulator in the system. Finally, energy delivered to the load, $E_{deliver}$, is defined as

$$E_{deliver} = E_{resuable} + E_{ss}. \tag{8}$$

The overall energy efficiency from the battery to the load in the hybrid system is given by

$$\eta_{system} = \frac{E_{deliver}}{E_{stored}} = \frac{1}{E_{stored}} \int_0^{t_{end}} i_o v_o \, dt, \tag{9}$$

where E_{stored}, $E_{deliver}$, i_o, v_o, and t_{end} denote the stored energy in the battery, delivered energy to the load, load current, load voltage, and service life of the hybrid system, respectively.

The energy density of the system may be calculated as

$$\rho_{hybrid} = \frac{E_b + E_s}{H_b + H_s}, \tag{10}$$

where E_b, E_s, H_b and H_s denote the amount of stored energy in the battery, amount of stored energy in the supercapacitor, volume of the battery and volume of the supercapacitor, respectively. Finally, we get the deliverable energy density which is given by

$$\rho_{deli} = \eta_{system} \cdot \rho_{hybrid}. \tag{11}$$

Based on the definition of the system efficiency, delivered energy, volumetric energy density, and deliverable energy density, we can formulate an optimization problem for designing battery-supercapacitor hybrid system using the constant-current regulator as follows.

Problem 1. Determine (C_s, i_{chg}) to achieve the maximum deliverable energy density $\rho_{deliver}$ for given a battery and load profile, considering the maximum voltage rating of the supercapacitor as well as current and voltage ratings of the converters as the constraints. □

Key parameters of the supercapacitors in the hybrid system are the voltage rating and capacitance. These parameters are directly related to the energy transfer efficiency and energy density of the proposed system. The capacitance value of the supercapacitor affects the efficiency due to its filtering effect on the pulsed load. Moreover, the volume of the supercapacitor is determined by its capacitance value and voltage rating. Because different amounts of charging current result indifferent steady states, the value of charging current results in different requirements for the voltage rating

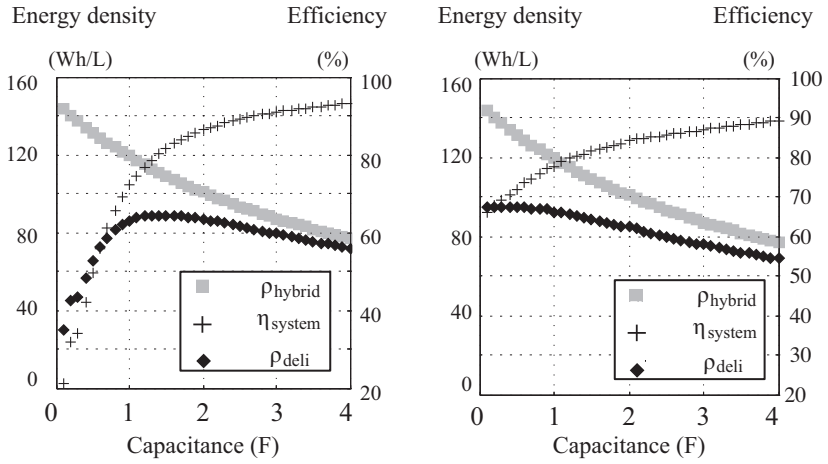

Fig. 8. System efficiency, energy density, and deliverable energy density of the parallel connection and the constant-current regulator-based system with pulsed load. (a) Parallel connection. (b) Constant-current regulator-based system.

for the supercapacitor. These two design parameters, i.e., the supercapacitor capacitance and charging current, also strongly influence the efficiency of the regulator. The operating conditions of the switching DC–DC converters, battery, and supercapacitor should be considered as constraints.

4.4. Optimization algorithm

Algorithm 1 *(Algorithm for constant-current regulator based hybrid system design space exploration).*

Input: Load profile: (i_{peak}, i_{idle}, t_{on}, t_{off}),
Specification of battery, supercapacitor and switching DC–DC converter
output: C_s, v_{max}, i_{chg}
1 **Calculate** minimum required capacitance $C_{s,min}$, maximum operating voltage $v_{max,min}$, and maximum charging current $i_{chg,max}$ according to the operating range of the DC–DC converter;
2 **Set** $C_s = C_{s,min}$ and $\rho_{deli,max} = 0$;
3 **Set** $v_{max} = v_{max,min}$ and $i_{chg} = i_{chg,max}$;
4 **Calculate** v_{ss} and $\overline{v_s}$ by (6);
5 **Calculate** $\overline{P_{converter}}$ with $\overline{v_s}$ and i_{chg} during steady-sate operation by (3);
6 **If** $\frac{\overline{dP_{conduction}}}{di_{chg}} > -\frac{\overline{dP_{gate}}}{di_{chg}}$ and $\overline{v_s} < v_{max}$ **Then** $i_{chg} = i_{chg} - \Delta i_{chg}$ **go to** 4;
7 **If** $\overline{v_s} = v_{max}$ & $\rho_{deli}(C_s, v_{max}, i_{chg}) - \rho_{deli}(C_s, v_{max}, 0) > \rho_{deli}(C_s, v_{max} + v_{unit}, i_{chg}) - \rho_{deli}(C_s, v_{max}, i_{chg})$ by (7)–(11) **Then** $v_{max} = v_{max} + v_{unit}$ **go to** 4;
8 **If** $\rho_{deli}(C_s, v_{max}, i_{chg}) > \rho_{deli,max}$ **Then** $\rho_{deli,max} = \rho_{deli}$ and $C_s = C_s + \Delta C_s$ **Go to** 3;
9 **Return** C_s, v_{max}, and i_{chg};

We develop a simulation environment including the Li-ion battery, supercapacitor, regulator, and load to solve the aforesaid optimization problem by simulation. We measure the characteristics of the actual devices to extract the parameters for the models. Based on the simulation environment, we develop a design space exploration algorithm which derives the capacitance and the maximum operating voltage of the supercapacitor array as well as the magnitude of charging current. We need to perform time-consuming SPICE-level simulation to obtain ρ_{deli}. The proposed algorithm greatly reduces size of search space by exploiting the characteristics of the proposed system. We need to explore the design space for three variables: capacitance of supercapacitor array, C_s, maximum operating voltage of supercapacitor array, v_{max}, and output of constant-current regulator, i_{chg}.

In practice, we can find a wide range of capacitance values in commercially available supercapacitors, but their maximum terminal voltage is fixed to 2.5 V or 2.7 V. This maximum voltage level is regarded as an industrial standard for the supercapacitor manufacturing. We use the parameter of currently available supercapacitors for the simulation, and change the maximum terminal voltage and capacitance of the supercapacitor array by connecting unit supercapacitors in series or parallel. For example, we need to connect 2 supercapacitors in series when we need up to 3 V terminal voltage. Therefore, we use a virtually continuous C_s using very small ΔC_s similar to i_{chg} and discrete maximum terminal values according to v_{max} to calculate the volume of the supercapacitor array.

We obtain optimal i_{chg} and v_{max} for given C_s without full-time simulation using the relationship among i_{chg}, v_s, and $P_{converter}$ which is given by (3) and (7) to reduce the design space exploration time. We further reduce search space for C_s by considering the concavity of ρ_{deli} versus C_s. We cannot directly use this for discrete C_s, but use it as a termination condition for search.

Algorithm 1 describes the proposed algorithm. We initially obtain the minimum required capacitance $C_{s,min}$ and the maximum operating voltage $v_{max,min}$ according to the operating range of the DC–DC converter. $C_{s,min}$ is determined by the maximum input voltage of the DC–DC converter and $v_{max,min}$ is determined by the minimum input voltage of the DC–DC converter. We can estimate the energy flow of the supercapacitor for a given load profile considering the conversion efficiency. The energy flow causes the terminal voltage fluctuation of the supercapacitor. The peak voltage of the terminal voltage fluctuation must be within the operating range of the DC–DC converters. Therefore, $i_{chg,max}$ is determined by the output range of the constant-current regulator.

First, we obtain the optimal i_{chg} for given C_s and v_{max}. For given C_s, we can estimate steady-state voltage v_{ss} by (6) and calculate average supercapacitor terminal voltage $\overline{v_s}$ by

$$\overline{v_s} = \frac{1}{t_{i+1} - t_i} \int_{t_i}^{t_{i+1}} v_s dt. \tag{12}$$

$\overline{v_s}$ is inversely proportional to i_{chg} when the delivered power is the same. In practice, we usually use the same switch for the power switch and synchronous switch of the DC–DC converter to simplify the driver circuit and make a symmetrical switching operation. Therefore, in (6), we assume that $P_{conduction}$ is only proportional to the square of i_{chg} and P_{gate} is only proportional to $\overline{v_s}$ without loss of generality. With this assumption, we obtain optimal i_{chg} by decreasing it from the initial maximum until $P_{conduction}$ decrement is equal to P_{gate} increment or $\overline{v_s}$ reaches v_{max}. We increase the v_{max} only when the gain in ρ_{deli} that comes from v_{max} increase is greater than maximum possible gain originated from i_{chg} decrease. We repeat

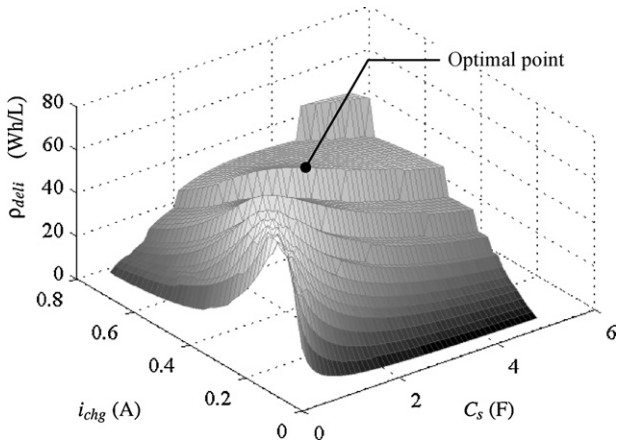

Fig. 9. Design space exploration result by simulation.

above process as increasing C_s. It stops and returns the optimization result when ρ_{deli} starts to decrease.

4.5. Design space exploration

First, to show a motivational example, we obtain the energy efficiency and deliverable energy density of the system by simulation using the parameters of the Li-ion battery and supercapacitor. We use a pulse current of 10 s period, and 10% duty cycle whose discharging rate is 10 C. From Fig. 8(a), the energy efficiency, η_{system}, increases as the capacitance of the supercapacitor increases. However, ρ_{deli}, decreases as the capacitance increases due to the fact that the energy density of the supercapacitor is much lower than that of the battery.

Next, we perform design space exploration to find the capacitance of the supercapacitor and the charging current for the proposed hybrid system. We use the battery model and the switching DC–DC converter model with the extracted parameters in Table 1. The simulation result of the energy density on C_s-i_{chg} domain is shown in Fig. 9. We use NessCap ESHSR0010C0-002R7 1 F supercapacitor as a unit for the array. We obtain the optimal design parameters of C_s = 2.5 F and i_{chg} = 0.41 A, from the deliverable energy density perspective using the proposed algorithm. Optimization is performed within the range of capacitance from 0.1 to 5 F and the charging current from 0.1 to 0.7 A. The maximum charging current is 2 C rate.

As we can see in Fig. 9, the deliverable energy density shows stepwise concave shape as C_s increases due to the system efficiency and the energy density. The value of the charging current affects the voltage rating of the supercapacitor and the converter efficiency simultaneously. If we apply a small charging current, we need a high steady-state voltage which results in the supercapacitor volume to be increased. On the other hand, a large charging current causes an excessive converter conductive loss.

5. Implementation

Commercial regulator ICs feature some attractive functions such as multi-chemistry battery support, USB compatibility, and cell protection and monitoring. However, it is difficult to find regulators that satisfy all of our requirements. First, we need a wide output voltage range (unlike batteries, supercapacitors have a wide range of output voltage variation according to their SOC). Unfortunately, commercial regulators are commonly designed for the stacked battery cells which show a limited range of output voltage. Next, we need high maximum charging current because the supercapacitors have a higher charging current rating compared to that of batteries.

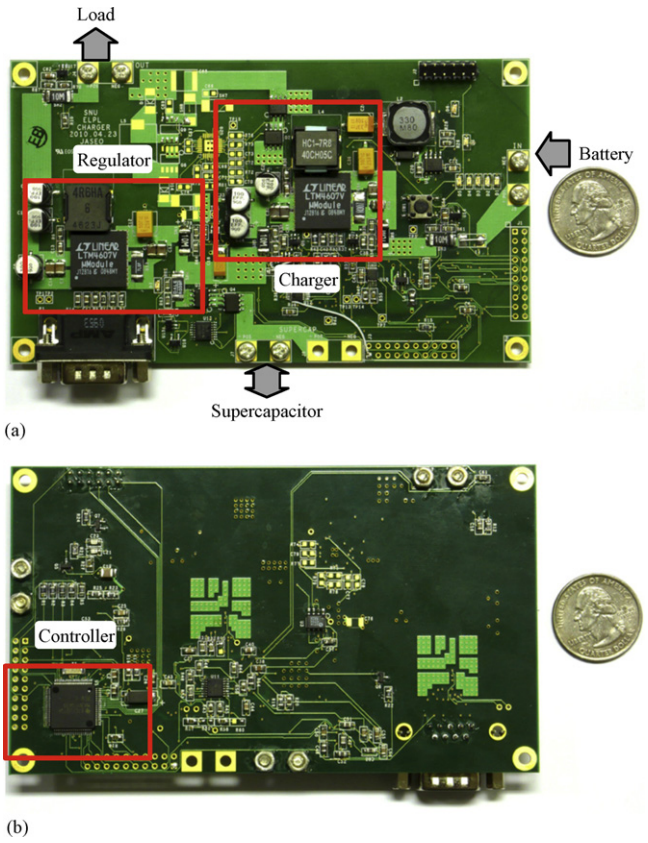

Fig. 10. Hybrid power controller board. (a) Top. (b) Bottom.

Conventional battery and supercapacitor regulators have a limited maximum charging current capability. Of course, high conversion efficiency is also essential.

We design a new regulator circuit using a high-efficiency switching buck-boost converter LTM4607 from Linear Technology [24]. The LTM4607 has an input voltage range of from 4.5 to 36 V, an output voltage range from 0.8 to 24 V, and delivers up to 5 A of current. It is specified in the manufacturer's datasheet that the conversion efficiency reaches up to 98%. The LTM4607 is originally designed as a DC–DC converter which generates only a constant–voltage. It has a voltage feedback input to regulate output voltage by adjusting the inductor current. We modify the feedback circuit so that the feedback voltage reflects the magnitude of output current. We did not change the converter topology, and always

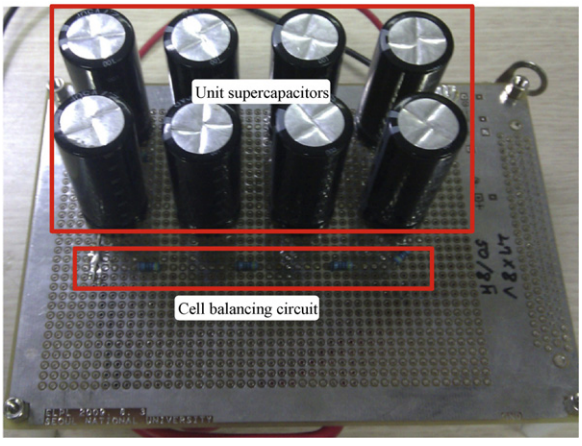

Fig. 11. Supercapacitor array.

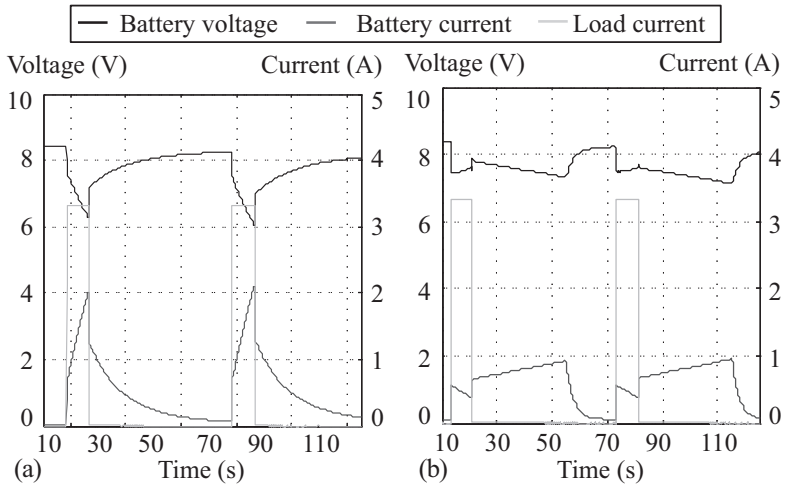

Fig. 12. Load current, battery voltage, and battery current of the parallel connection and the constant-current regulator-based system with pulsed load. (a) Parallel connection. (b) Constant-current charger based system.

use the converter within the specified safe operating range of the LTM4607 module. Therefore, only the switching duty D in power model (3) is affected by the feedback loop modification. The other physical parameters presented in Table 1 are basically the same whether it is in the constant-current operation or constant–voltage operation.

We also use another LTM4607 to supply a regulated voltage to the load as the recommended circuit design by the manufacturer. It has a wide range of input voltage and output voltage enough to accept the supercapacitor terminal voltage as an input. In addition it exhibits high conversion efficiency over a wide range of output currents.

We use an ultra low-power 16-bit microprocessor MSP430 from Texas Instruments as the controller. It has a 12-channel 12-bit ADC and a 2-channel 12-bit DAC required for measurement and control. The control software task has a 1 ms of execution period. Fig. 10 shows the implemented hybrid power system board prototype.

We implement the supercapacitor array using the unit supercapacitor. We use passive cell balancing circuit and the implemented array is partially reconfigurable. Fig. 11 shows the supercapacitor array.

6. Experiment

As shown in Fig. 12, the constant-current regulator allows one to achieve smoother supercapacitor charging current with the same supercapacitor capacitance. We can see that the average discharging current in the proposed hybrid architecture is much smaller than that in the parallel connection configuration. Accordingly, we obtain a higher overall energy density for the electrical energy storage system while ensuring that the deliverable energy to the load is maximized.

Fig. 13 shows the voltage and current change of two different battery-supercapacitor hybrid systems when a pulsed load is applied. We use the battery and supercapacitor described in Section 4.2. The 2.5 F supercapacitor is composed of four serially connected 10 F supercapacitors. The pulse has 3.5 A peak current, which corresponds to 10 C, 10 s period, and 10% duty cycle. Fig. 13(a) is the result of the parallel connection, and Fig. 13(b) is the result of the proposed hybrid architecture. Evidently, the proposed architecture achieves 7.7% service time improvement which corresponds to the same amount of the deliverable energy density gain where the same battery and supercapacitor setup is used.

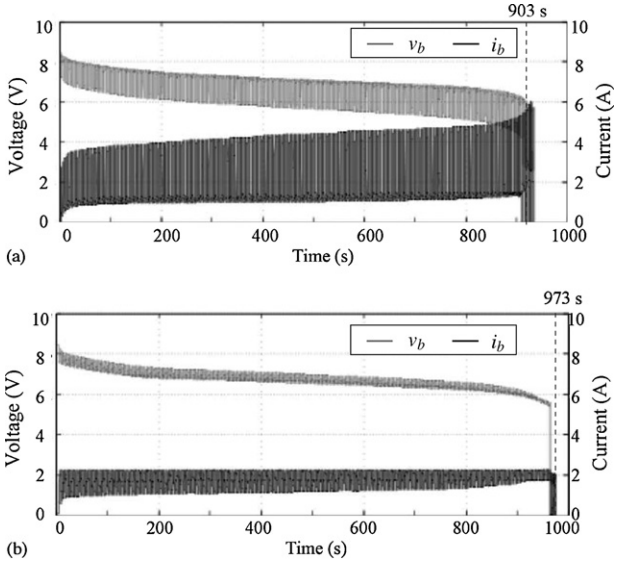

Fig. 13. Voltage and current measurements while discharging 350 mAh 2-cell Li-ion battery with 2.5 F supercapacitor. The load pulse has 10 C rate peak, 10 s period, and 10% duty. (a) Parallel connection architecture. (b) Proposed hybrid architecture.

7. Conclusion

The battery-supercapacitor hybrid can reduce the loss due to the rate capacity effect for the modern portable electronics which have a highly fluctuating load profile. Conventional parallel connection battery-supercapacitor hybrid needs a large supercapacitor so as to reduce the battery's peak discharging current enough to relieve the rate capacity effect on the battery. However, the large supercapacitor drastically degrades the overall available energy density which is one of the most critical constraints for the power source of portable electronics. By isolating the battery from supercapacitor, proposed constant-current regulator-based hybrid system relieves the rate capacity effect with smaller supercapacitor than the parallel connection. We derive the optimal steady-state condition of the system to balance the power from the battery to the load for given periodic pulsed load. Experimental results show that the proposed hybrid system achieves up to 7.7% deliverable energy density improvement compared to the parallel connection.

References

[1] D. Shin, Y. Wang, Y. Kim, J. Seo, M. Pedram, N. Chang, Battery-supercapacitor hybrid system for high-rate pulsed load applications, in: Proceedings of Design Automation and Test in Europe (DATE), 2011.
[2] F. Simjee, P. Chou, Everlast: long-life, supercapacitor-operated wireless sensor node, in: Proceedings of International Symposium on Low Power Electronics and Design, 2006.
[3] J. Luo, N.K. Jha, Battery-aware static scheduling for distributed real-time embedded systems, in: Proceedings of Design Automation Conference 2001, 2001.
[4] M. Pedram, C.-Y. Tsui, Q. Wu, An integrated battery-hardware model for portable electronics, in: Proc. of Asia and South Pacific Design Automation Conference, 1999.
[5] M. Pedram, Q. Wu, Design considerations for battery-powered electronics, IEEE Trans. VLSI Syst. 10 (5) (2002) 601–607.
[6] C.F. Chiasserini, R.R. Rao, Routing protocols to maximize battery efficiency, in: Proceedings of 21st Century Military Communications Conference (MILCOM 2000), 2000.
[7] S. Pay, Y. Baghzouz, Effectiveness of battery-supercapacitor combination in electric vehicles, in: Proceedings of IEEE Bologna Power Tech Conference, 2003.
[8] P. Thounthonga, S. Raelb, B. Davatb, Energy management of fuel cell/battery/supercapacitor hybrid power source for vehicle applications, J. Power Sources, 2009.
[9] T.B. Atwater, P.J. Cygan, F.C. Leung, Man portable power needs of the 21st century: I. Applications for the dismounted soldier. II. Enhanced capabilities through the use of hybrid power sources, J. Power Sources, 2000.
[10] C.E. Holland, J.W. Weidner, R.A. Dougal, R.E. White, Experimental characterization of hybrid power systems under pulse current loads, J. Power Sources, 2002.
[11] R. Dougal, S. Liu, R. White, Power and life extension of battery-ultracapacitor hybrids, IEEE Trans. Compon. Pack. Technol., 2002.
[12] G. Sikha, B.N. Popov, Performance optimization of a battery-capacitor hybrid system, J. Power Sources, 2004.
[13] Gold Peak Industries, GP batteries datasheet: Model GP1051L35, 2011.
[14] Harris, AN/VRC-103(V)1, AN/VRC-103(V)2 specification, 2008.
[15] P. Rong, M. Pedram, An analytical model for predicting the remaining battery capacity of Lithium-ion batteries, IEEE Trans. VLSI Syst., 2006.
[16] D. Rakhmatov, Battery voltage modeling for portable systems, in: ACM TODAES, 2009.
[17] L. Benini, G. Castelli, A. Macii, E. Macii, M. Poncino, R. Scarsi, Discrete-time battery models for system-level low-power design, IEEE Trans. VLSI Syst., 2001.
[18] M. Chen, G. Rincon-Mora, Accurate electrical battery model capable of predicting runtime and *I–V* performance, IEEE Trans. Energy Convers, 2006.
[19] W. Lajnef, J.M. Vinassa, O. Briat, S. Azzopardi, E. Woirgard, Characterization methods and modelling of ultracapacitors for use as peak power sources, J. Power Sources, 2007.
[20] Y. Choi, N. Chang, T. Kim, DC–DC converter-aware power management for low-power embedded systems, IEEE Trans. Comput.-Aid. Des., 2007.
[21] A. Chu, P. Braatz, Comparison of commercial supercapacitors and high-power Lithium-ion batteries for power-assist applications in hybrid electric vehicles: I. initial characterization, J. Power Sources, 2002.
[22] E. Vilar, R. Dougal, Study of pulsed-current loading of direct methanol fuel cells using a new time-domain model based on bi-functional methanol oxidation kinetics, J. Power Sources 169 (2) (2007) 276–287.
[23] NessCap, NessCap ultracapacitor datasheet: ESHSR-0010C0-002R7, 2003.
[24] Linear Technology, LTM4607: 36 V in, 24 V out high efficiency buck-boost DC/DC μModule, 2008.